Blood flow directs arterial-venous remodeling through Notch activation and endothelial cell migration.

Bart Weijts[1,2], Edgar Gutierrez[3], Semion K Saikin[4], Ararat J Ablooglu[2], David Traver[1], Alex Groisman[3] and Eugene Tkachenko[2#]

[1]Department of Cellular and Molecular Medicine, University of California-San Diego, La Jolla, CA 92093, USA
[2]Department of Medicine, University of California-San Diego, La Jolla, CA 92093, USA
[3]Dpartment of Physics, University of California-San Diego, La Jolla, CA 92093, USA
[4]Department of Chemistry and Chemical Biology, Harvard University, Cambridge, MA 02138, USA

Correspondence should be addressed to ET (etkachenko@ucsd.edu), DT (dtraver@ucsd.edu) and AG (agroisman@ucsd.edu).

Arteries and veins are lined by arterial and venous endothelial cells (ECs), which are functionally distinct[1,2]. During embryonic development, vascular remodeling transforms some arteries into veins. Arterial and venous embryonic ECs have the plasticity to transdifferentiate into each other [3–6], suggesting that the transformation of arteries to veins may be accompanied by trans-differentiation of ECs. Here, we show that transformation of arterial intersegmental vessels (aISVs) into veins occurs without trans-differentiation, by the displacement of arterial ECs by venous ECs, and requires normal blood flow. At the same time, the establishment of blood flow prevents neighboring aISVs from transforming into veins via the upregulation of Notch signaling in these aISVs. We propose that through these two processes, blood flow facilitates the transformation of the all-arterial trunk vasculature into a functional vascular network with near equal numbers of arteries and veins.

Embryonic vascular remodeling connects arterial and venous vascular trees and is essential for establishing a supply of blood to all parts of the body. The intersegmental vasculature of the vertebrate trunk is initially formed by arterial ECs that sprout from the dorsal aorta (DA) and migrate dorsally between somites to ultimately connect with each other to form the dorsal longitudinal anastomotic vessel (DLAV). To establish circulation through this arterial trunk vasculature, about half of the aISV are transformed to venous ISVs (vISVs) through fusion with venous sprouts derived from the posterior cardinal vein (PCV) (Fig.1a). Arterial and venous ECs are molecularly distinct, with Notch signaling

being a major hallmark of arterial identity[2]. Notch signaling is required for arterial specification and maintenance [2,7,8] and has been suggested to be involved in vascular remodeling[9,10].

Here, we used the zebrafish embryo model to explore the role of Notch signaling in vascular remodeling at the level of individual ISVs. Just before the beginning of remodeling (26 hpf), we administrated the γ-secretase inhibitor dibenzazepine (DBZ)[11], which prevents the cleavage and the release of the transcriptionally active Notch intracellular domain (NICD). Chemical blockade of Notch signaling with DBZ [in *Tg(flt4:YFP; flt1enh:tdTomato)*[9] embryos] resulted in a significant majority of ISVs being connected to the PCV (Fig.1b, d). The expression of the Notch ligand *delta-like 4* (*dll4*), which triggers a strong Notch response[12], is restricted to the arterial endothelium[13] and has been shown to be essential for normal arterial angiogenesis[14,15]. To determine if *dll4* is involved in the Notch dependent transformation of arteries to veins, we abrogated *dll4* expression by injecting either a *dll4* guide-RNA and *CAS9* mRNA or reduced it by using a low dose of *dll4* morpholino oligonucleotide (MO). In both cases, we observed that a reduction in *dll4* expression resulted in increased proportion of vISVs (Fig.1b,d). Next, we ectopically activated Notch signaling by driving NICD specifically within arterial ECs [in *Tg(dll4:GAL4; UAS:NICD)*], and observed a reduced proportion of vISVs (Fig.1c,d). Taken together, our results suggest that Dll4-dependent Notch signaling in aISVs prevents the transformation of these vessels into veins.

Blood flow has been proposed to play an important role in vasculature remodeling[16], but molecular mechanisms have not been identified. Hydrodynamic flow was shown to upregulate Notch signaling in arterial ECs in mouse embryos and *in vitro*[17,18]. We acutely reduced the blood flow in *Tg(TP1:D2GFP)* Notch reporter embryo using 0.04% tricaine methanesulfonate (2×MS222) that lowered the heart rate and blood flow[19], leading to reduced Notch signaling in arterial ECs (Fig.1e). (Neural Notch signaling was unaffected). The same 2xMS222 treatment also resulted in a significant increase in the proportion of vISVs (Fig.1f, g). The results of these two experiments suggest that weaker than normal blood flow results in reduced Notch signaling, ultimately leading to more aISVs being transformed into vISV.

Our classification of an ISV as venous has been based on whether it is connected to the PCV. To properly function, veins need to be lined with venous ECs. At the time when an ISV connects to the PCV it becomes a vISV which is still populated with arterial ECs. As time passes, vISVs become populated with venous ECs all the way up to the DLAV (brackets in Fig.1b, SFig.1c-d). Interestingly, in Notch inhibited embryos, even by the end of the remodeling, only the most ventral parts of vISV were populated with venous ECs (brackets in Fig.1b). These animals also had a reduced blood flow through the vISVs (as judged by a reduced number of passing erythrocytes), which was presumably due to a disproportionally large ratio of vISVs to aISVs. We also found that complete blockage or partial reduction of blood flow resulted in a similar phenotype, with ISVs connected to the PCV but having venous ECs in only the most ventral parts (Fig.1f and SFig.1f, g). These observations suggest that normal blood flow is required to complete the formation of functional vISVs.

To investigated the effects of flow on ECs, we performed *in vitro* experiments in microfluidics perfusion chambers applying a range of shear stresses (τ) to confluent human umbilical venous endothelial cells (HUVECs) and human umbilical arterial endothelial cells (HUAECs). Both types of ECs migrated against flow when τ was sufficiently large (Fig.2, SFig.2a, Movies 1,2). Changes in the direction of EC migration in response to the flow correlated with changes in their planar polarization, an indicator of migratory bias of ECs (Fig.2d, Movie 3)[20]. The times it took for HUVECs to establish directional migration and planar polarization after the inception of flow both decreased as τ increased, and the ultimate migration velocity of HUVECs increased with τ. These experiments suggest that blood flow may cause upstream migration of ECs and the migration slows or stops when blood flow weakens.

To determine if blood flow also causes EC migration *in vivo*, we tracked differentially labeled arterial and venous ECs in embryonic zebrafish trunk. We found that after the initiation of blood flow through vISVs, venous ECs started to migrate from the PCV into vISVs displacing arterial ECs (Fig.3a-d, Movies 4,5,6). This observation suggests, that complete population of newly formed vISVs with venous ECs occurs by migration against the blood flow, resulting in invasion of venous ECs and displacement of arterial ECs.

Our results can be explained by the following model. When a venous sprout originated from the PCV fuses with an ISV, it causes the initiation of blood flow through this ISV towards the PCV and blood flow through the two nearest neighbor ISVs away from the DA. The latter blood flow activates Notch signaling in these two ISVs, thereby preventing their transformation into veins and protecting their arterial identity (Fig.3e). Blood flow through next neighboring ISVs is not strong enough to sufficiently activate Notch signaling and to protect them from transforming into vISVs. As a result, every other ISV remains arterial and, at the end of the vascular remodeling, the ratio of vISVs to aISVs is 50:50. At the same time, blood flow induces upstream migration of ECs, leading to the displacement of arterial ECs in the vISV by venous ECs (Fig.3e). The displacement of ECs of one type by ECs of another through directed migration may also be involved in remodeling of other vascular beds.

Materials and Methods

Zebrafish husbandry

Zebrafish (*Danio rerio*) were maintained according to the guidelines of the UCSD Institutional Animal Care and Use Committee. The following zebrafish lines have been previously described: *Tg(fli1a:GFP)^{y1}* (ref.[21]), *Tg(UAS:lifeactGFP)^{mu271}* (ref.[22]), *Tg(dll4:Gal4FF^{hu10049})* (ref.[13]), Tg(UAS:tagRFP) (ref.[23]), *Tg(flt4:YFP)* (ref.[10]), *Tg(flt1enh:tdTomado)* (ref.[10]), *Tg(fli1a:lifeactCherry)* (ref.[24]), *Tg(EPV.Tp1-Mmu.Hbb:d2GFP)^{mw43}* (ref.[25]) abbreviated as *Tg(Tp1:d2GFP)*, *Tg(UAS:myc-Notch1a-intra)^{kca3}* (ref.[26]) *abbreviated as Tg(UAS:NICD), Tg(flk:KAEDE).*

Morpholino and RNA injections

Embryos were injected at the one-cell stage with 1 nl morpholino oligonucleotides (MOs), 100ng mRNA or 100ng gRNA*. Delta like 4 (dll4)* splice-site MO (GeneTools) (5-TGATCTCTGATTGCTTACGTTCTTC-3)[10] *at* 1 ng/nl; *cardiac troponin T (tnnt2)* ATG MO (GeneTools) (5-CATGTTTGCTCTGATCTGACACGCA-3) at 4ng/nl. Capped *CAS9 mRNA* was synthesized from linearized pCS2+ constructs using the mMessage mMachine SP6 kit (Ambion, AM1340), and was injected into embryos at a concentration of 100ng. A gene specific oligo containing the SP6 promoter and *dll4* guide RNA sequence was annealed to the constant oligo as previously described[27]. *dll4* gRNA1*:* ATTTAGGTGACACTATAGGTAGTTTTTTAGGCAAACTGTTTTAGAGCTAGAAATAGCAAG. *dll4* gRNA2: ATTTAGGTGACACTATAGTGCCTTAACGCCAGTGCTGGTTTTAGAGCTAGAAATAGCAAG. gRNAs were transcribed using the SP6 MEGAscript kit (Ambion, AM1330).

Constructs

H2b-EGFP and H2b-mCherry in SIN18.hPGK.eGFP.WPRE lentiviral vector were gifts from J.H. Price[28]. GFP-α-tubulin in pRRL.PPT.CMV lentiviral vector was kindly provided by O. Pertz. Lentiviruses were produced as described[28].

Microscopy

Live imaging was done with environmentally controlled microscopy systems based on a Nikon TE 2000 brightfield microscope[20,29,30], a Perkin Elmer UltraView spinning disk confocal microscope and a Leica TSP LSM 5 confocal microscope. For all imaging, embryos were embedded into an imaging chamber (SFig.1a,b) submerged in 0.4% low melting agarose in E3

medium containing 1xMS222 at a temperature of 28.5 °C. Imaging was subsequently done with either 20x/0.75, 40x/1.3 or 63x/1.40 objectives. Experiments on HUVECs and HUAECs on fibronectin coated glass cover slips in microfluidic devices were done as previously described [20,29]. Tracking and polarization analysis of ECs *in vitro* was done using ImagePro 6.1 (MediaCybernatics, Bethesda, MD) and home-built applications in Matlab (Mathworks, Natick, MA).

Microfluidic devices

PDMS-based microfluidic devices and zebrafish imaging dishes were fabricated as previously described[29].

Cell Culture

Culturing of ECs *in vitro.* Culturing of HUVECs and HUAECs (Lonza, Basel, Switzerland) was done as previously described[29].

Statistical analysis

Statistical analysis was performed using SPSS 20 (IBM). Mann-Whitney U test was used for statistical analysis of two groups, unequal variances, and unpaired t test for two groups, equal variances. Kruskal-Wallis test was used for statistical analysis of multiple groups, equal varuances, and 1-way ANOVA, for multiple groups, unequal variances. Dunns post-hoc test was used for pairwise multiple comparisons. P values < 0.05 were considered significant.

References

1. Dela Paz, N. G. & D'Amore, P. A. Arterial versus venous endothelial cells. *Cell Tissue Res* **335,** 5–16 (2009).
2. Torres-Vázquez, J., Kamei, M. & Weinstein, B. M. Molecular distinction between arteries and veins. *Cell Tissue Res* **314,** 43–59 (2003).
3. Othman-Hassan, K. *et al.* Arterial identity of endothelial cells is controlled by local cues. *Dev Biol* **237,** 398–409 (2001).
4. Red-Horse, K., Ueno, H., Weissman, I. L. & Krasnow, M. A. Coronary arteries form by developmental reprogramming of venous cells. *Nature* **464,** 549–553 (2010).
5. Buschmann, I. *et al.* Pulsatile shear and Gja5 modulate arterial identity and remodeling events during flow-driven arteriogenesis. *Development* **137,** 2187–2196 (2010).
6. Le Noble, F. *et al.* Flow regulates arterial-venous differentiation in the chick embryo yolk sac. *Development* **131,** 361–375 (2004).
7. Quillien, A. *et al.* Distinct Notch signaling outputs pattern the developing arterial system. *Development* **141,** 1544–1552 (2014).
8. Lawson, N. D. *et al.* Notch signaling is required for arterial-venous differentiation during embryonic vascular development. *Development* **128,** 3675–3683 (2001).
9. Geudens, I. *et al.* Role of delta-like-4/Notch in the formation and wiring of the lymphatic network in zebrafish. *Arterioscler Thromb Vasc Biol* **30,** 1695–1702 (2010).
10. Hogan, B. M. *et al.* Vegfc/Flt4 signalling is suppressed by Dll4 in developing zebrafish intersegmental arteries. *Development* **136,** 4001–4009 (2009).
11. Van Es, J. H. *et al.* Notch/gamma-secretase inhibition turns proliferative cells in intestinal crypts and adenomas into goblet cells. *Nature* **435,** 959–963 (2005).
12. Gama-Norton, L. *et al.* Notch signal strength controls cell fate in the haemogenic endothelium. *Nat Commun* **6,** 8510 (2015).
13. Hermkens, D. M. A. *et al.* Sox7 controls arterial specification in conjunction with hey2 and efnb2 function. *Development* **142,** 1695–1704 (2015).
14. Shutter, J. R. *et al.* Dll4, a novel Notch ligand expressed in arterial endothelium. *Genes Dev* **14,** 1313–1318 (2000).

15. Leslie, J. D. *et al.* Endothelial signalling by the Notch ligand Delta-like 4 restricts angiogenesis. *Development* **134,** 839–844 (2007).
16. Isogai, S., Lawson, N. D., Torrealday, S., Horiguchi, M. & Weinstein, B. M. Angiogenic network formation in the developing vertebrate trunk. *Development* **130,** 5281–5290 (2003).
17. Jahnsen, E. D. *et al.* Notch1 is pan-endothelial at the onset of flow and regulated by flow. *PLoS ONE* **10,** e0122622 (2015).
18. Masumura, T., Yamamoto, K., Shimizu, N., Obi, S. & Ando, J. Shear stress increases expression of the arterial endothelial marker ephrinB2 in murine ES cells via the VEGF-Notch signaling pathways. *Arterioscler Thromb Vasc Biol* **29,** 2125–2131 (2009).
19. Lenard, A. *et al.* In vivo analysis reveals a highly stereotypic morphogenetic pathway of vascular anastomosis. *Dev Cell* **25,** 492–506 (2013).
20. Tkachenko, E. *et al.* The nucleus of endothelial cell as a sensor of blood flow direction. *Biology open* **2,** 1007–1012 (2013).
21. Lawson, N. D. & Weinstein, B. M. In vivo imaging of embryonic vascular development using transgenic zebrafish. *Dev Biol* **248,** 307–318 (2002).
22. Helker, C. S. M. *et al.* The zebrafish common cardinal veins develop by a novel mechanism: lumen ensheathment. *Development* **140,** 2776–2786 (2013).
23. Kawakami, K. *et al.* A transposon-mediated gene trap approach identifies developmentally regulated genes in zebrafish. *Dev Cell* **7,** 133–144 (2004).
24. Wakayama, Y., Fukuhara, S., Ando, K., Matsuda, M. & Mochizuki, N. Cdc42 mediates Bmp-induced sprouting angiogenesis through Fmnl3-driven assembly of endothelial filopodia in zebrafish. *Dev Cell* **32,** 109–122 (2015).
25. Clark, B. S. *et al.* Loss of Llgl1 in retinal neuroepithelia reveals links between apical domain size, Notch activity and neurogenesis. *Development* **139,** 1599–1610 (2012).
26. Scheer, N. & Campos-Ortega, J. A. Use of the Gal4-UAS technique for targeted gene expression in the zebrafish. *Mech Dev* **80,** 153–158 (1999).

27. Gagnon, J. A. *et al.* Efficient mutagenesis by Cas9 protein-mediated oligonucleotide insertion and large-scale assessment of single-guide RNAs. *PLoS ONE* **9,** e98186 (2014).
28. Kita-Matsuo, H. *et al.* Lentiviral vectors and protocols for creation of stable hESC lines for fluorescent tracking and drug resistance selection of cardiomyocytes. *PLoS ONE* **4,** e5046 (2009).
29. Tkachenko, E., Gutierrez, E., Ginsberg, M. H. & Groisman, A. An easy to assemble microfluidic perfusion device with a magnetic clamp. *Lab Chip* **9,** 1085–1095 (2009).
30. Tkachenko, E. *et al.* Protein kinase A governs a RhoA-RhoGDI protrusion-retraction pacemaker in migrating cells. *Nat Cell Biol* **13,** 660–667 (2011).

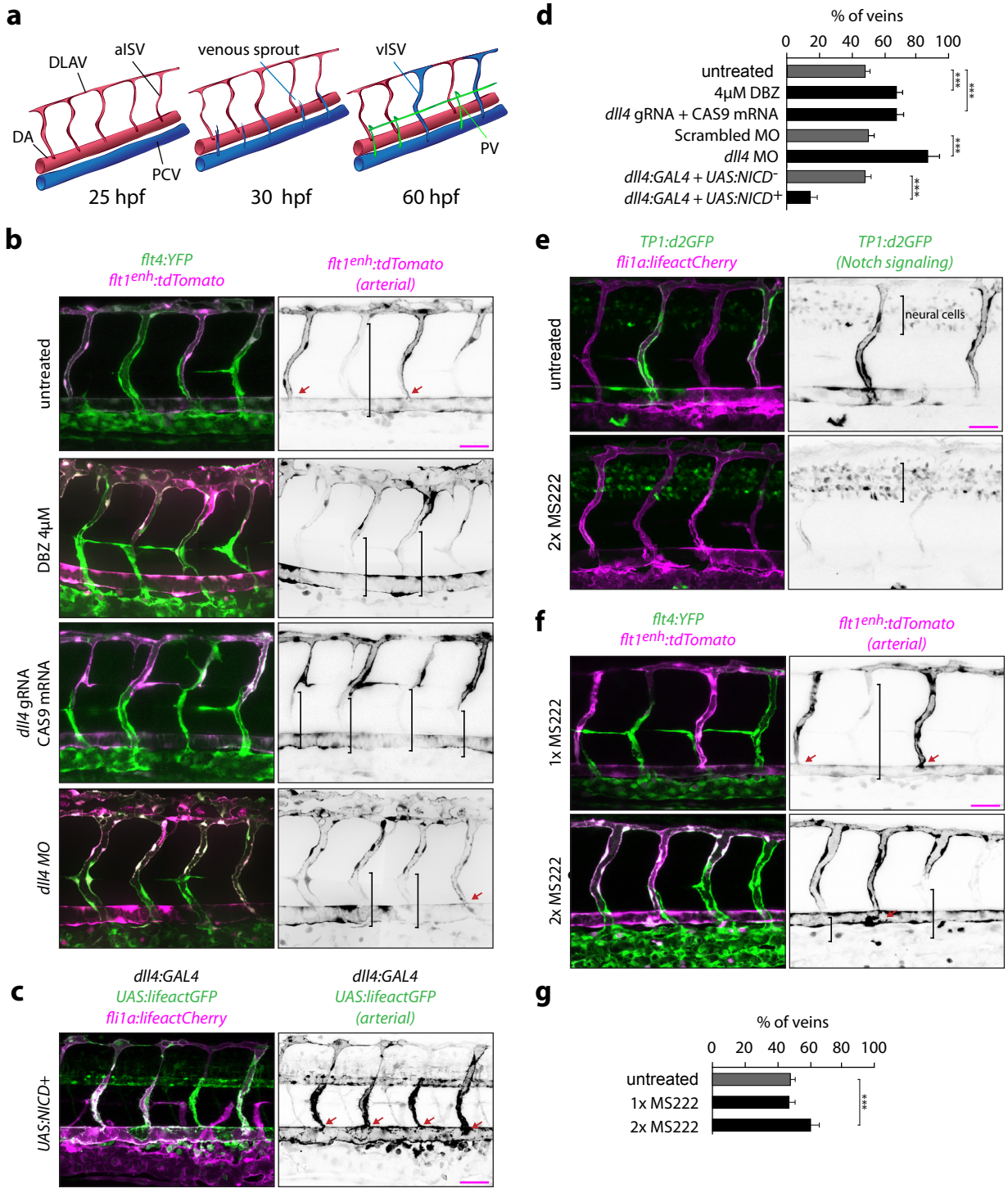

Figure 1

Figure 1. **Remodeling of intersegmental vasculature is regulated by arterial Notch signaling and requires normal blood flow.**
Panels (b), (c), (e), and (f) show lateral images of zebrafish embryos at 60 hpf. For right panels in (b), (c), and (f) red arrows point to aISVs and brackets indicate regions of vISVs without arterial ECs. Scale bars are 25 μm. All numbers are averages ± SEM from three independent experiments.'***' indicates P<0.001.
a) Schematic overview of intersegmental vasculature remodeling. DA - dorsal aorta, PCV - posterior cardinal vein, DLAV - dorsal longitudinal anastomotic vessel, aISV/vISV – arterial/venous intersegmental vessel, PV - parachordal vessel.
b) Venous ECs are labeled with YFP and arterial ECs with YFP and Tomado. Embryos were untreated, treated with 4μM DBZ at 26 hpf, injected at the single cell stage with 100 ng *dll4* guide RNA and 100ng *CAS9* mRNA, or injected at the single cell stage with 1ng *dll4* MO.
c) Arterial but not venous ECs have upregulated Notch signaling due to expression of Notch Intracellular Domain (NICD). Arterial ECs express lifeactCherry and venous ECs express lifeactCherry and lifeactGFP.
d) Ratios of vISVs and aISVs in embryos with perturbed Notch signaling. *n≥65* per condition from three independent experiments.
e) Embryos expressing Notch signaling reporter [destabilized GFP under control of a Notch- responsive promoter] and lifeactCherry in ECs were treated at 26 hpf with 1x or 2x MS222. Note, that 2x MS222 resulted in reduced Notch signaling in arterial vasculature but not in the neural tube.
f) Venous ECs labeled with YFP and arterial EC labeled with YFP and Tomado. 1x or 2x MS222 was applied at 26 hpf.
g) Ratios of vISVs and aISVs in embryos with blood flow reduced as a result of 2x MS222 treatment. *n≥63* per condition from three independent experiments.

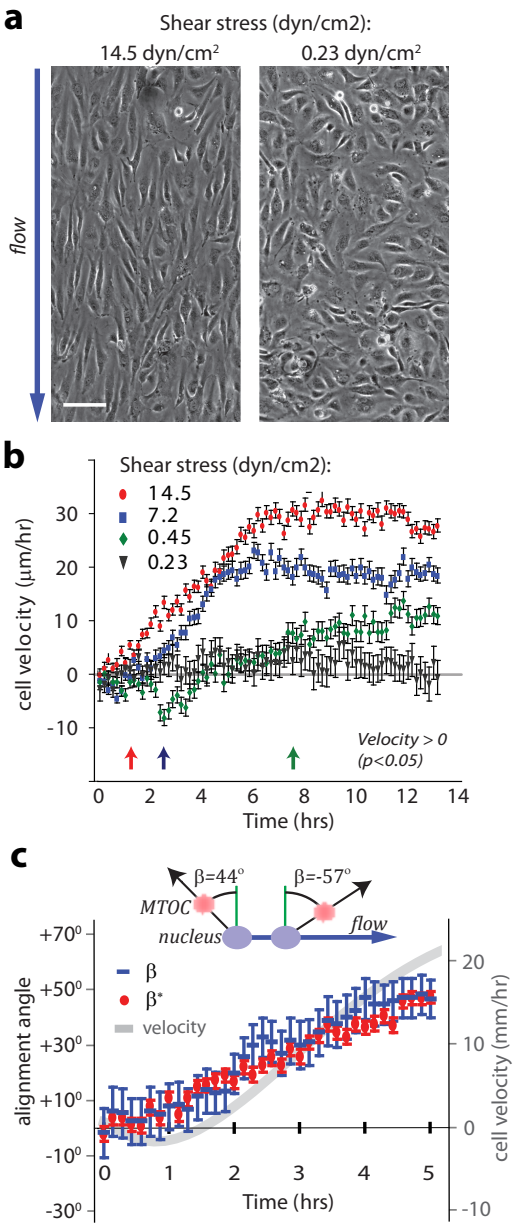

Figure 2

Figure 2. **Migration of ECs against hydrodynamic flow.**
a) Phase images of confluent HUVECs after 10 hrs under laminar flows with shear stresses of 14.5 and 0.23 dyn/cm^2. Scale bar is 100 μm.
b) Average velocities of upstream migration for HUVECs exposed to different shear stresses as functions of time after the inception of the shear flows (n=250 to 600 for individual shear stresses). *Arrows* at the bottom (colors correspond to those of the velocity data points) indicate the time points at which the migration of cells against the flow becomes statistically significant (average upstream velocity becomes positive with $p<0.05$). c) Positions of MTOC and nuclei in individual HUVECs and their instantaneous velocities were monitored for 300 min after the exposure to flow with a shear stress $\tau = 7.2$ dyn/cm^2. *Blue dashes* show the values of the polarization angle, β, with 90° corresponding to polarization against the flow and β = -90° - polarization along the flow. *Red circles* show the values of the migration angle, β*, with 90° corresponding to migration against the flow and β* = -90° - migration along the flow. Grey line (ordinate on the right) show the average cell migration velocity upstream. Data in (b) and (c) is representative of 3 independent experiments. Error bars are SEM.

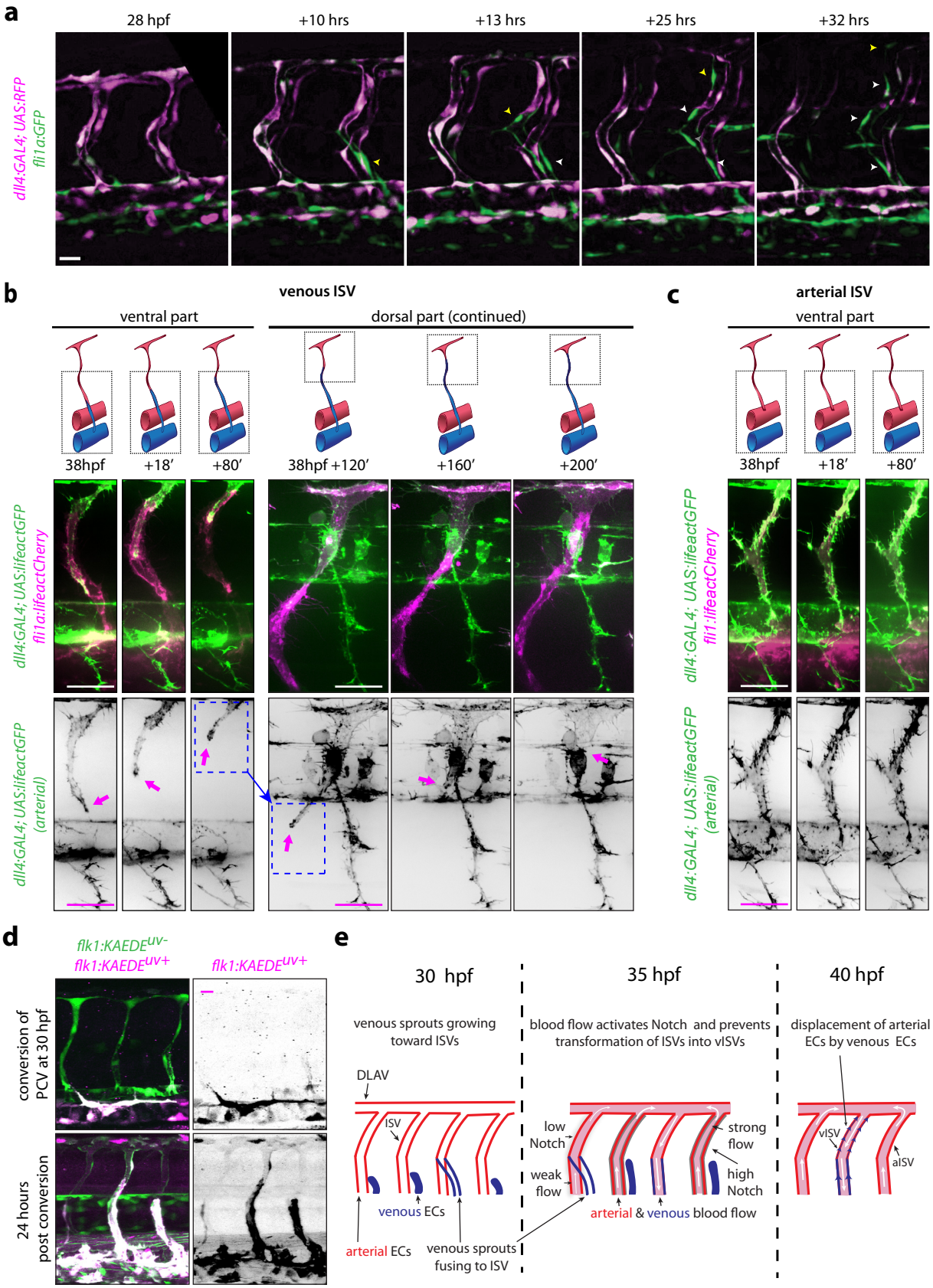

Figure 3

Figure 3. **Blood flow promotes displacement of arterial ECs by venous ECs in vISVs.** Lateral images of blood vessels in zebrafish embryos at different time points between somites 14 and 15 with anterior side facing left. Scale bars are 25 μm.

a) Venous ECs are labelled with GFP and arterial ECs are labelled with GFP and mCherry. Individual venous ECs invading into a vISV are highlighted by *arrows*.

b,c) Venous ECs express lifeactCherry and arterial ECs express lifeactCherry and lifeactGFP. b) Magenta arrows highlight the retraction of arterial ECs from an vISV towards the DLAV. c) In an aISV, there is no detectable EC migration.

d) ECs express photo-convertible (green-to-red) fluorescent protein KAEDE. ECs in the PCV were photo-converted and imaged at 30 hpf (white in the left panels and black in the right) and then imaged at 54 hpf, when some of them invaded ISVs.

e) A model explaining how blood flow-induced Notch signaling and endothelial migration enable the remodeling of all-arterial intersegmental vasculature into a network with 1:1 ratio of arteries and veins.

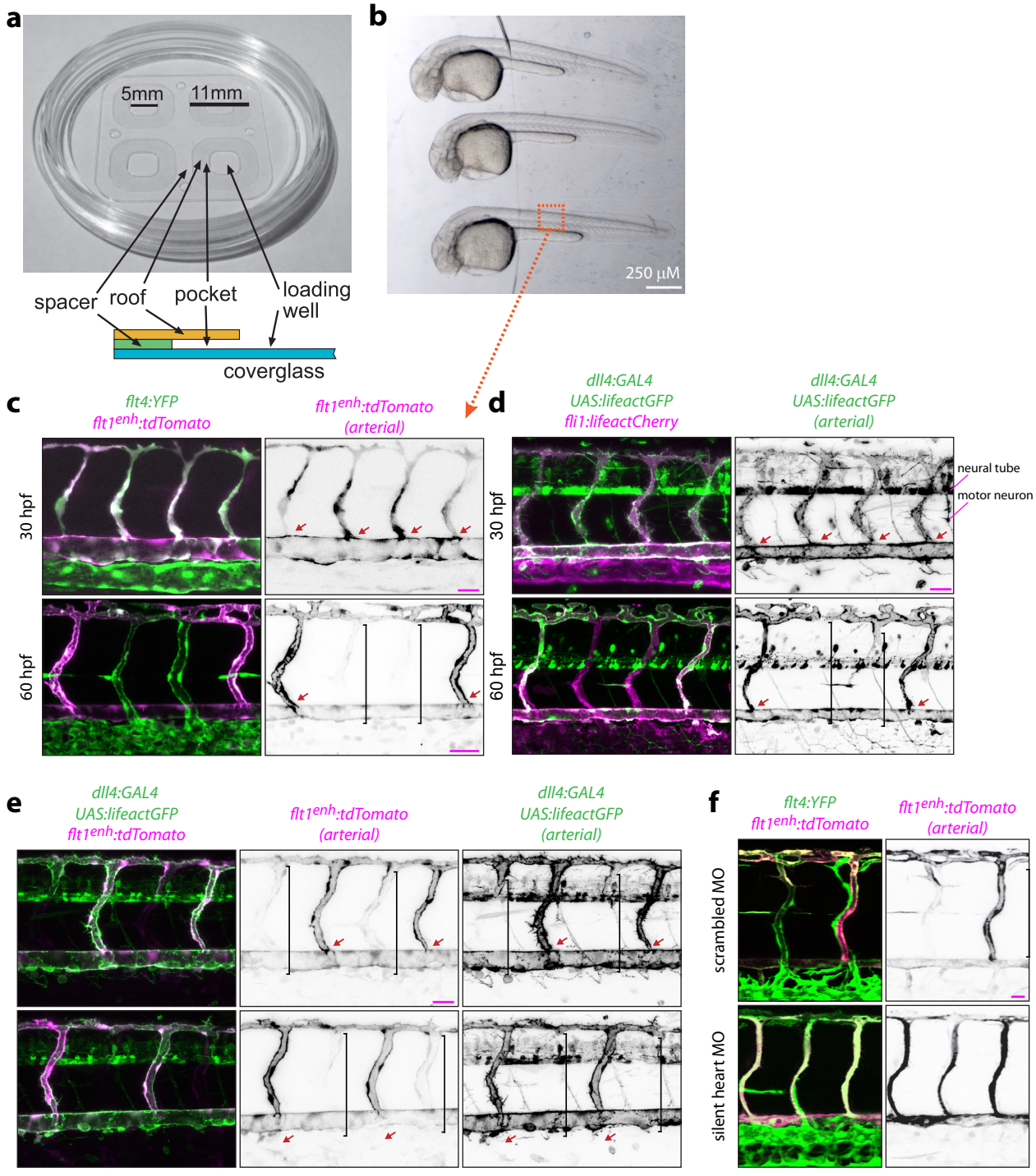

Supplementary Figure 1

Supplementary Figure 1. **Remodeling of intersegmental vasculature requires normal blood flow.**

a) Multiwell dish for high-resolution lateral imaging of zebrafish embryos.

b) Large scale view of three 24 hpf zebrafish embryos in a well of the imaging dish.

c-f) Lateral images of zebrafish embryos. In monochrome panels, red arrows point to arterial ISVs and brackets indicate regions of venous ISVs that do not have arterial ECs. Scale bars are 25 μm.

c) Venous ECs are labeled with YFP and arterial ECs with YFP and Tomado.

d) Venous ECs express lifeactCherry and arterial ECs express lifeactCherry and lifeactGFP.

e) Arterial ECs express lifeactGFP and Tomado; 60 hpf.

f) Venous ECs are labeled with YFP and arterial ECs with YFP and Tomado; 60 hpf. Embryos were injected at the single cell stage with 1ng of silent heart (*tnnt2)* MO.

g) Average growth (%) for control (n=2) and *tnnt2a* (n=3) morpholino-injected 32 hpf embryos over 24 hrs. Growth was calculated by measuring the distance between somites 14 and 16. Error bars are SD.

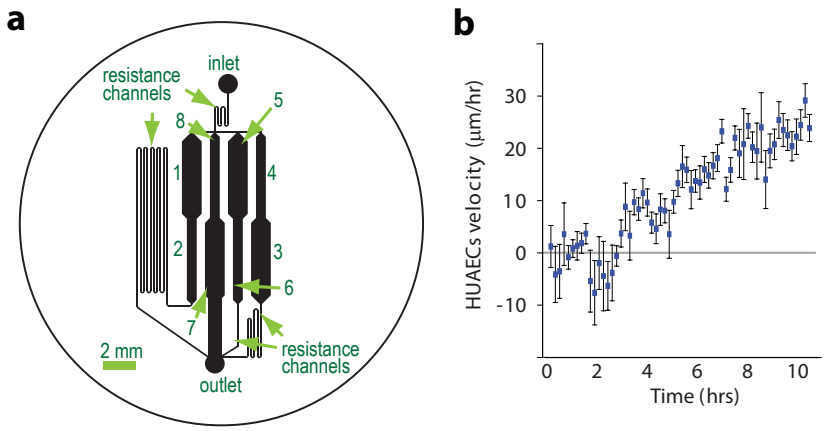

Supplementary Figure 2. **Polarization and migration of ECs exposed to shear flow in the microfluidic system.**

a) Schematics of the microfluidic device. The device has 8 separate test regions, with a uniform shear stress at the substrate in each region and ~2 fold change in the shear stress, τ, between regions with consecutive numbers (total of ~128 fold between 1 and 8, from low to high).

b) Average velocities of migration of HUAECS against the flow as functions of time from the moment of their first exposure to flow with a shear stresses τ = 8 dyn/cm^2 (n=230). Error bars are SEM.

MOVIES

Movie 1. **Migration of HUVECs exposed to a high shear stress in the microfluidic model.** Phase-contrast images of HUVECs exposed to a shear stress τ =14.5 dyn/cm^2 were acquired every 10 min. Direction of the flow was from left to right. Frame rate is 6 per sec (1 sec = 1 hr). Scale bar is 50 μm.

Movie 2. **Migration of HUVECs exposed to a low shear stress in the microfluidic model.** Phase-contrast images of HUVECs exposed to a shear stress τ =0.23 dyn/cm^2 were acquired every 10 min. Direction of the flow was from left to right. Frame rate is 6 per sec (1 sec = 1 hr). Scale bar is 50 μm.

Movie 3. **Flow-induced changes in the planar polarization and migration of HUVECs in the microfluidic model.** Positions of MTOC and nuclei in individual HUVECs were monitored for 300 min after their exposure to flow with a shear stress τ = 7.2 dyn/cm^2. The direction of flow is from left to right. *Left panel* shows fluorescence images (with an inverted grayscale) of a fragment of a microchannel with ECs expressing GFP-α-tubulin. *Right panel* shows phase contrast images of the same area. Individual cells are labeled by color-coded arrows. In the left panel, the arrows show the direction of cell polarization and their color indicates the polarization angle, β, with red corresponding to 90° (polarization against the flow) and blue corresponding to β = -90° (polarization along the flow). In the right panel, the arrows show the direction of cell migration and their color represents the angle between the directions of migration and flow, β*, with red corresponding to 90° (migration against the flow) and blue corresponding to β* = -90° (migration along the flow). The dials in the top left corners show color-coded polarization angle, β (*left panel*), and migration angle, β* (*right panel*) averaged over all cells in the field of view. Images were acquired every 10 min. Frame rate is 3 per sec (1 sec = 30 min). Scale bar is 30 μm.

Movie 4. **Displacement of arterial ECs by venous ECs in vISVs.** All ECs express lifeactCherry (*magenta*) and arterial ECs also express lifeactGFP (*green*). The field of view between somites 14 and 16. Images are taken every 30 min. Frame rate is 2 per sec (1 sec = 1 hr). Scale bar is 30 μm.

Movie 5. **Retraction of art\erial ECs from a venous ISV towards the DLAV (*ventral part*).** All ECs express lifeactCherry (*magenta*) and arterial ECs also express lifeactGFP (*green*). Intensity of GFP is inverted for better contrast. Images were taken every 2.2 min. Frame rate is 4.5 per sec (6 sec = 1 hr). Scale bar is 25 μm.

Movie 6. **Retraction of arterial ECs from a venous ISV towards the DLAV (*dorsal part*).** All ECs express lifeactCherry (*magenta*) and arterial ECs also express lifeactGFP (*green*). Intensity of GFP is inverted for better contrast. Images were taken every 1.3 min. Frame rate is 7.6 per sec (6 sec = 1 hr). Scale bar is 25 μm.

Movie 7. **Arterial ECs in an arterial ISV (*ventral part*).** All ECs express lifeactCherry (*magenta*) and arterial ECs also express lifeactGFP (*green*). Intensity of GFP is inverted for better contrast. Images were taken every 2.2 min. Frame rate is 4.5 per sec (6 sec = 1 hr). Scale bar is 25 μm.

AUTHOR CONTRIBUTIONS

BW, AJA and ET designed and performed the experiments with zebrafish. EG, AG and ET designed experiments in microfluidic devices. ET performed microfluidic experiments. SKS, BW and ET analyzed the data. BW, AG and ET wrote the manuscript. DT edited the manuscript and reviewed the data.